

Quantum molecular dynamics simulations for the nonmetal-to-metal transition in fluid helium

André Kietzmann, Bastian Holst, and Ronald Redmer
Universität Rostock, Institut für Physik, D-18051 Rostock, Germany

Michael P. Desjarlais and Thomas R. Mattsson
Pulsed Power Science Center, Sandia National Laboratories, Albuquerque, New Mexico 87185-1186, USA
 (Dated: July 26, 2018)

We have performed quantum molecular dynamics simulations for dense helium to study the nonmetal-to-metal transition at high pressures. We present new results for the equation of state and the Hugoniot curve in the warm dense matter region. The optical conductivity is calculated via the Kubo-Greenwood formula from which the dc conductivity is derived. The nonmetal-to-metal transition is identified at about 1 g/cm^3 . We compare with experimental results as well as with other theoretical approaches, especially with predictions of chemical models.

PACS numbers: 05.70.Ce, 52.25.Fi, 52.25.Kn, 52.65.Yy, 64.30.+t

Hydrogen and helium are by far the most abundant elements in nature. The investigation of their phase diagram, especially at extreme conditions of pressure and temperature, is not only of fundamental interest but also an indispensable prerequisite for astrophysics. For instance, thermophysical properties of hydrogen-helium mixtures determine the structure and evolution of stars, White Dwarfs, and Giant Planets [1, 2, 3]. The detection of Jupiter-like planets orbiting neighboring stars [4] has initiated a renewed interest in planetary physics. All planetary models require an input of accurate equation of state data in order to solve the hydrostatic equations for a rotating compact object. While the limiting cases of low and high densities are well understood within chemical and plasma models, the intermediate region is much more complex. There, a nonmetal-to-metal transition occurs in both hydrogen and helium at pressures of several megabar and temperatures of few eV which implies a strong state-dependence of the interparticle interactions and, thus, also of the thermodynamic variables. In this paper, we study this *warm dense matter* region where the uncertainties in the equation of state data, both experimentally and theoretically, are greatest.

A lot of effort has been done to understand the behavior of warm dense hydrogen [5, 6]. Although the simplest element in the periodic table, the transition of a non-conducting molecular liquid to an atomic or plasma-like conducting fluid at high pressure is still not fully understood [7, 8, 9]. Helium seems to be a much simpler system for the study of the high-pressure behavior since no dissociation equilibrium between molecules and atoms interferes with the ionization equilibrium, and the first (24.6 eV) and second ionization energy (54.4 eV) are well separated. Surprisingly, only few experimental and theoretical studies exist for warm dense helium [10, 11, 12].

In this paper, we perform the first comprehensive *ab initio* study of the high-pressure behavior of helium. We determine the equation of state (EOS) in the warm dense matter region by means of quantum molecular dynamics (QMD) simulations. The Hugoniot curve is derived and compared with experimental points [13], other *ab initio* calculations [14], as well as with results of efficient chemical models [10, 11, 12]. Finally, we calculate the dynamic conductivity via the Kubo-Greenwood formula and derive the static conductivity and compare with shock wave experimental data [20]. We locate the nonmetal-to-metal transition in the high-pressure phase diagram and discuss the related plasma phase transition (PPT).

QMD simulations are a powerful tool to calculate the structural, thermodynamic, and optical properties of warm dense matter in a combined first-principles approach. Details of this method have been described elsewhere [17, 21, 22, 23].

We have performed *ab initio* molecular dynamics simulations employing a finite temperature Fermi occupation of the electronic states using Mermin's finite temperature density functional theory (FT-DFT) [24]. The implementation of the QMD method comes from VASP (Vienna Ab Initio Simulation Package), a plane wave density functional code developed at the University of Vienna [25]. All electrons are treated quantum mechanically on the level of DFT. The electronic wave function is relaxed at each QMD step, which assumes decoupled electronic and ionic time scales. We have chosen a simulation box with 32 to 64 atoms and periodic boundary conditions. The electron wave functions are modeled using the projector augmented wave (PAW) potentials [26] supplied with VASP [25]. These PAW potentials enable more accurate results for conductivity calculations compared with other pseudopotentials. The exchange correlation functionals

are calculated within generalized gradient approximation (GGA). Our most accurate calculations were done using the GGA parameterization of PBE [27]. The convergence of the thermodynamic quantities in QMD simulations is of significant importance [28]. We have chosen a plane wave cutoff E_{cut} at 700 eV where the pressure is converged to within 2%.

Performing QMD simulations to calculate the EOS of He only the Γ point was used for the representation of the Brillouin zone. Calculations for Al have shown that it is not recommended to calculate higher-order \mathbf{k} -point sets [17]. Furthermore, the mean value point (1/4, 1/4, 1/4) was used for conductivity calculations.

Our simulations were performed for a canonical ensemble where the temperature, the volume of the simulation box, and the particle number in the box are conserved quantities during a QMD run. To keep the temperature on a predefined level, the ion temperature is regulated by a Nosé-Hoover thermostat and the electronic temperature is fixed by Fermi weighting the occupation of bands [25]. After about hundred time steps the system is equilibrated and the subsequent 400 to 1000 time steps are taken to calculate pressures, energies and other quantities as averages over this simulation period.

First we present results for the thermal and caloric EOS of warm dense helium in Figs. 1 and 2. The isotherms of the pressure and the internal energy behave very systematically with temperature and density and show no indications of an instability such as the PPT at lower temperatures, contrary to results derived within the chemical picture [10, 11, 12]. For instance, the EOS of Winisdoerffer and Chabrier (WC) [12] is based on a free energy minimization schema for a mixture of helium atoms, single and double charged ions, and free electrons. Correlations are taken into account based on effective two-particle potentials. It agrees well with our QMD results for the pressure up to about 1 g/cm³ and for ultra-high densities above about 50 g/cm³. However, this chemical model shows a systematic trend to lower pressures in the intermediate, strongly coupled region where the QMD results already approach an almost temperature-independent behavior as characteristic of a degenerate electron gas. These results underline the significance of *ab initio* calculations for warm dense matter states and will have a strong impact on calculations of planetary interiors [29]. Furthermore, we can identify the region where efficient chemical models are applicable in favor of time-consuming *ab initio* calculations.

Based on this EOS data, we have determined the Hugoniot curve via the condition

$$(E - E_0) = \frac{1}{2}(P + P_0)(V_0 - V), \quad (1)$$

which relates all final states of a shock wave experiment (E, P, V) with the initial state (E_0, P_0, V_0) . In our calculations we have used the values $E_0 = 20$ J/g,

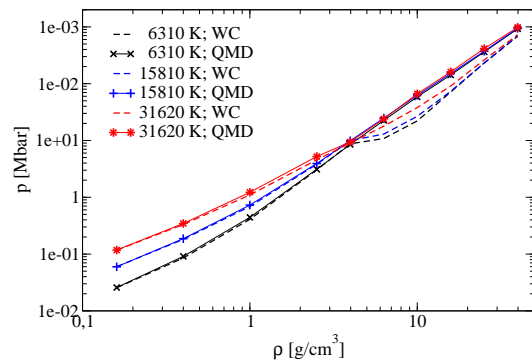


FIG. 1: Pressure isotherms in comparison with the WC free energy model [12].

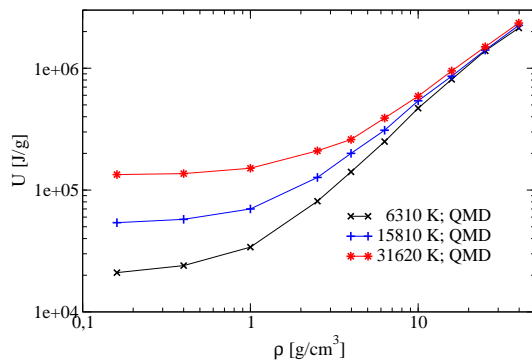


FIG. 2: Isotherms of the internal energy.

$T_0 = 4$ K, $P_0 = 1$ bar $\ll P$, and $V_0 = 32.4$ cm³/mol ($\rho_0 = 0.1235$ g/cm³) for the first shock and $E_1 = 57$ kJ/g, $T_1 = 15.000$ K, $P_1 = 190$ kbar, and $V_1 = 9.76$ cm³/mol ($\rho_1 = 0.41$ g/cm³) for the second shock. We compare our results with double-shock experiments of Nellis *et al.* [13], with recent DFT-MD calculations of Militzer [14], and with two chemical models [12, 30] in Fig. 3.

A very good agreement is found with the double-shock experiments as well as with the other theoretical Hugoniot curves up to about 1 g/cm³ which results from the accordance of the EOS data up to this density as mentioned above. A central problem in this context is the value and location of the maximum compression ratio η_{max} . The chemical model FVT_{id}⁺ [30] is based on fluid variational theory and considers an ideal ionization equilibrium in addition. This model predicts a value of 5.5 at 375 GPa and 50.000 K if the second shock of the experiment is taken as initial state. Militzer [14] found a maximum compression of 5.24 at 360 GPa and 150.000 K for the principal Hugoniot starting at (E_0, P_0, V_0) by using an EOS composed of zero-Kelvin DFT-MD results accounting for excited states for lower temperatures as shown in Fig. 3 and Path Integral Monte Carlo (PIMC) data in the high-temperature limit. Note that only a finite-temperature DFT calculation yields the self-consistent thermal ground state of the system, which is

not equivalent to applying a thermal occupation of the empty electronic states (“excited states”) obtained in a zero-Kelvin electronic structure calculation as performed in [14]; for details, see [31].

The QMD simulations were performed up to 1.5 g/cm^3 , 350 GPa, and 60.000 K where the maximum compression ratio has not been reached yet. For still higher temperatures the number of bands increases drastically beyond the scope of our computer capacity. Besides PIMC simulations [14], orbital-free DFT methods may be applicable in that high-temperature region [32]. Interestingly, the maximum compression ratio for helium ($\eta_{\text{max}} \geq 5$) is greater than that for hydrogen ($\eta_{\text{max}} = 4.25$); see e.g. [6] for a more detailed discussion.

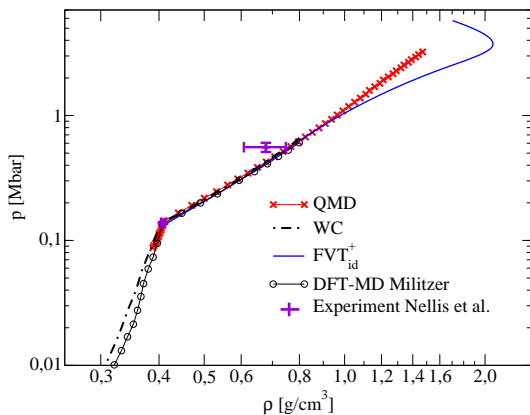


FIG. 3: Hugoniot curve for helium: QMD results are compared with double-shock experiments of Nellis *et al.* [13], zero-Kelvin DFT-MD results of Militzer [14] accounting for excited states, and two chemical models WC [12] and FVT_{id}⁺ [30].

The dynamic conductivity $\sigma_{\mathbf{k}}(\omega)$ for one \mathbf{k} point is derived from the Kubo-Greenwood formula [15, 16]

$$\sigma_{\mathbf{k}}(\omega) = \frac{2\pi e^2 \hbar^2}{3m^2 \omega \Omega} \sum_{j=1}^N \sum_{i=1}^N \sum_{\alpha=1}^3 [F(\epsilon_{i,\mathbf{k}}) - F(\epsilon_{j,\mathbf{k}})] \times |\langle \Psi_{j,\mathbf{k}} | \nabla_{\alpha} | \Psi_{i,\mathbf{k}} \rangle|^2 \delta(\epsilon_{j,\mathbf{k}} - \epsilon_{i,\mathbf{k}} - \hbar\omega), \quad (2)$$

where e is the electron charge and m its mass. The summations over i and j run over N discrete bands considered in the electronic structure calculation for the cubic supercell volume Ω . The three spatial directions are averaged by the α sum. $F(\epsilon_{i,\mathbf{k}})$ describes the occupation of the i th band corresponding to the energy $\epsilon_{i,\mathbf{k}}$ and the wavefunction $\Psi_{i,\mathbf{k}}$ at \mathbf{k} . δ must be broadened because of the discrete eigenvalues resulting from the finite simulation volume [17]. Integration over the Brillouin zone is done by sampling special \mathbf{k} points [18],

$$\sigma(\omega) = \sum_{\mathbf{k}} \sigma_{\mathbf{k}}(\omega) W(\mathbf{k}), \quad (3)$$

where $W(\mathbf{k})$ is the weighting factor for the respective \mathbf{k} point. Calculations are usually done at the mean value point [19].

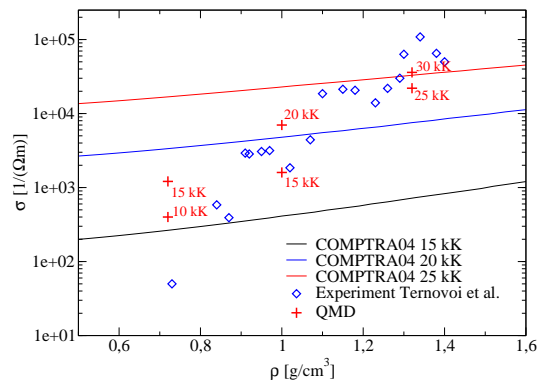


FIG. 4: QMD results for the static conductivity are compared with shock-wave experiments of Ternovoi *et al.* [20] between $(15 - 25) \times 10^3 \text{ K}$ and isotherms of the COMPTRA04 model [34]; temperatures are indicated.

The dc conductivity follows from Eq. (2) in the limit $\omega \rightarrow 0$. We compare with isentropic compression experiments of Ternovoi *et al.* [20] performed in the range $(15 - 25) \times 10^3 \text{ K}$ and predictions of the partially ionized plasma model COMPTRA04 [33, 34] in Fig. 4. The experimental points show a very strong increase between 0.7 and 1.4 g/cm^3 indicating that a nonmetal-to-metal transition occurs. Using the Mott criterion for the minimum metallic conductivity of $20000/\Omega\text{m}$ also for finite temperatures, this transition can be located at about 1.3 g/cm^3 . The QMD results reproduce the strong increase found experimentally very well except for the lowest density of 0.72 g/cm^3 where the experimental value is substantially lower than the QMD result.

The COMPTRA04 model [33, 34] calculates the ionization degree and, simultaneously, the electrical conductivity accounting for all scattering processes of free electrons in a partially ionized plasma. This approach is able to describe the general trends of the electrical conductivity with the density and temperature as found experimentally, see [35]. The isotherms displayed in Fig. 4 cover almost the range of the experimental points and agree also with the QMD data so that the nonmetal-to-metal transition is described qualitatively very well.

The strong influence of the temperature on the dc conductivity in this transition region can be seen by comparing the QMD results for two temperatures at the same density point; see Fig. 4. In order to exclude systematic errors from the experimental temperature determination, we have performed EOS calculations for the experimental points and compare typical values in Table I. A very good agreement is obtained so that the discrepancy in the conductivity data for the lowest density stems probably from the band gap problem of DFT. In order to solve this problem, DFT calculations beyond the GGA have to be performed by using, e.g., exact exchange formalisms [36] or quasi-particle calculations [37]. This is an important issue of future work devoted to the nonmetal-to-metal

transition.

TABLE I: Comparison of EOS data inferred from the experiment [20] and QMD data.

ρ [g/cm ³]	T [K]	p_{Exp} [kbar]	p_{QMD} [kbar]
0.73	16700	500	478
1.02	19400	900	892
1.38	23500	1685	1639

The origin of this nonmetal-to-metal transition can be elucidated by inspecting the variation of the density of states (DOS) along the path of the shock-wave experiments, see Fig. 5. For the lowest density of 0.72 g/cm³, a gap still exists in the DOS so that thermally activated electron transport occurs as in semiconductors. With increasing density, the gap region is slightly reduced. The main effect is, however, that electronic states fill up the region of the Fermi energy with increasing temperature so that a higher, metal-like conductivity follows, see also [8].

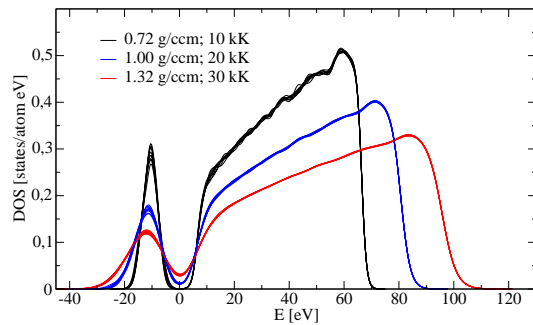


FIG. 5: DOS as function of the energy for three typical situations. The Fermi energy is located at zero.

In summary, we have determined the thermophysical properties of dense helium within an *ab initio* approach. The results show clearly the strong influence of quantum effects and correlations in the warm dense matter region. The nonmetal-to-metal transition occurs at about 1 g/cm³, in good agreement with shock wave experimental data. These new results will have a strong influence on models for planetary interiors.

We thank P.M. Celliers, V.E. Fortov, B. Militzer, V.B. Mintsev, and V.Ya. Ternovoi for stimulating discussions and for providing us with their data. This work was supported by the Deutsche Forschungsgemeinschaft within the SFB 652 and the grant mvp00006 of the supercomputing center HLRN.

[1] D. Saumon, G. Chabrier, and H.M. Van Horn, *Astrophys. J. Suppl. Ser.* **99**, 713 (1995).
 [2] V.Ya. Ternovoi *et al.*, *JETP Letters* **79**, 6 (2004).

[3] J. Vorberger, I. Tamblyn, B. Militzer, and S.A. Bonev, *Phys. Rev. B* (submitted).
 [4] M.A.C. Perryman, *Rep. Prog. Phys.* **63**, 1209 (2000). See also <http://exoplanet.eu> for up to date information.
 [5] D.A. Young and R. Cauble (Editors), *High Pressure Research* **16**, 281-400 (2000).
 [6] W.J. Nellis, *Rep. Prog. Phys.* **69**, 1479 (2006).
 [7] N.W. Ashcroft, *Phys. Rev. B* **41**, 10963 (1990); K. Johnson and N.W. Ashcroft, *J. Phys.: Condens. Matter* **10**, 11135 (1998).
 [8] L.A. Collins *et al.*, *Phys. Rev. B* **63**, 184110 (2001).
 [9] R. Redmer, G. Röpke, S. Kuhlbrodt, and H. Reinholz, *Phys. Rev. B* **63**, 233104 (2001).
 [10] A. Förster, T. Kahlbaum, and W. Ebeling, *Laser Part. Beams* **10**, 253 (1992); T. Kahlbaum and A. Förster, *Fluid Phase Equil.* **76**, 71 (1992).
 [11] M. Schlanges, M. Bonitz, and A. Tschtschjan, *Contrib. Plasma Phys.* **35**, 109 (1995).
 [12] C. Winisdoerffer and G. Chabrier, *Phys. Rev. E* **71**, 026402 (2005).
 [13] W.J. Nellis *et al.*, *Phys. Rev. Lett.* **53**, 1248 (1984).
 [14] B. Militzer, *Phys. Rev. Lett.* **97**, 175501 (2006).
 [15] R. Kubo, *J. Phys. Soc. Jpn.* **12**, 570 (1957).
 [16] D.A. Greenwood, *Proc. Phys. Soc. London* **71**, 585 (1958).
 [17] M.P. Desjarlais, J.D. Kress, and L.A. Collins, *Phys. Rev. E* **66**, 025401(R) (2002).
 [18] H.J. Monkhorst and J.D. Pack, *Phys. Rev. B* **13**, 5188 (1976).
 [19] A. Baldereschi, *Phys. Rev. B* **7**, 5212 (1973).
 [20] V.Ya. Ternovoi *et al.*, *AIP Conf. Proc.* **620**, 107 (2002).
 [21] M.P. Desjarlais, *Phys. Rev. B* **68**, 064204 (2003).
 [22] Y. Laudernet, J. Clérouin, and S. Mazevet, *Phys. Rev. B* **70**, 165108 (2004).
 [23] J. Clérouin *et al.*, P. Renaudin, Y. Laudernet, P. Noiret, and M.P. Desjarlais, *Phys. Rev. B* **71**, 064203 (2005).
 [24] N.D. Mermin, *Phys. Rev.* **137**, A1441 (1965).
 [25] G. Kresse and J. Hafner, *Phys. Rev. B* **47**, 558 (1993); **49**, 14251 (1994); G. Kresse and J. Furthmüller, *Phys. Rev. B* **54**, 11169 (1996).
 [26] P.E. Blöchl, *Phys. Rev. B* **50**, 17953 (1994); G. Kresse and D. Joubert, *Phys. Rev. B* **59**, 1758 (1999).
 [27] J.P. Perdew, K. Burke, and M. Ernzerhof, *Phys. Rev. Lett.* **77**, 3865 (1999).
 [28] A.E. Mattsson *et al.*, *Model. Simul. Mater. Sci. Eng.* **13**, R1 (2005).
 [29] D. Saumon and T. Guillot, *Astrophys. J.* **609**, 1170 (2004).
 [30] V. Schwarz, H. Juranek, and R. Redmer, *Phys. Chem. Chem. Phys.* **7**, 1990 (2005).
 [31] T.R. Mattsson and M.P. Desjarlais, *Phys. Rev. Lett.* **97**, 017801 (2006).
 [32] F. Lambert, J. Clérouin, and G. Zerah, *Phys. Rev. E* **73**, 016403 (2006).
 [33] S. Kuhlbrodt, B. Holst, and R. Redmer, *Contrib. Plasma Phys.* **45**, 73 (2005).
 [34] S. Kuhlbrodt *et al.*, *Contrib. Plasma Phys.* **45**, 61 (2005).
 [35] V.E. Fortov *et al.*, *J. Exp. Theor. Phys.* **97**, 259 (2003).
 [36] R.P. Muller and M.P. Desjarlais, *J. Chem. Phys.* **125**, 054101 (2006).
 [37] P. Rinke *et al.*, *New Journal of Physics* **7**, 126 (2005); S.V. Faleev *et al.*, *Phys. Rev. B* **74**, 033101 (2006).